DOI 10.5012/bkcs.2010.31.12.3579

Reaction of *Tri*-methylaluminum on Si (001) Surface for Initial Aluminum Oxide Thin-Film Growth

Dae-Hee Kim, Dae-Hyun Kim, Yong-Chan Jeong, Hwa-Il Seo,[†] and Yeong-Cheol Kim[*]

Department of Materials Engineering, [†]School of Information Technology, Korea University of Technology and Education, Cheonan 330-708, Korea. [*]E-mail: yckim@kut.ac.kr
Received April 26, 2010, Accepted September 27, 2010

We studied the reaction of *tri*-methylaluminum (TMA) on hydroxyl (OH)-terminated Si (001) surfaces for the initial growth of aluminum oxide thin-films using density functional theory. TMA was adsorbed on the oxygen atom of OH due to the oxygen atom's lone pair electrons. The adsorbed TMA reacted with the hydrogen atom of OH to produce a *di*-methylaluminum group (DMA) and methane with an energy barrier of 0.50 eV. Low energy barriers in the range of 0 - 0.11 eV were required for DMA migration to the inter-dimer, intra-dimer, and inter-row sites on the surface. A *uni*-methylaluminum group (UMA) was generated at each site with low energy barriers in the range of 0.21 - 0.25 eV. Among the three sites, the inter-dimer site was the most probable for UMA formation.

Key Words: *Tri*-methylaluminum, ALD, Silicon surface, Density function theory

Introduction

Increased gate oxide capacitance is needed to ensure the correct operation of metal-oxide semiconductor field-effect transistors (MOSFETs) as device dimensions shrink.[1] This can be achieved by decreasing the thickness of the gate oxide. However, the direct tunneling of electrons through the gate oxide becomes substantial for silicon oxide (SiO_2) layers below 1.2 nm thick.[2] Recently, high dielectric constant (high-*k*) materials have replaced SiO_2 as gate oxide materials.[3] Their necessary capacitance can be achieved with the thicker film, thereby avoiding the direct tunneling problem. Many experimental studies of high-*k* materials such as aluminum oxide (Al_2O_3), hafnium oxide (HfO_2), and zirconium oxide (ZrO_2) grown by atomic layer deposition (ALD) have been reported.[4-14] The ALD technique can control the uniformity and thickness of films on substrate surfaces at an atomic scale.[15,16] The important thing for the ALD process is the initial reaction between the molecule and surface, because it determines the high-*k*/surface interface structure.

Among high-*k* materials, Al_2O_3 has superior physical and electronic properties, such as large band gap (9 eV), reasonable dielectric constant (9), and high break down field (5 - 10 MV/cm).[7,17,18] Theoretical studies of the initial growth of Al_2O_3 thin-films on Si surfaces have been researched using first principles calculations.[19-23] Lee *et al.* deposited Al_2O_3 thin-films using *tri*-methylaluminum (TMA, $Al(CH_3)_3$) and H_2O as precursors on OH-terminated and H-terminated Si (001) surfaces.[24] They reported that the incubation period could be avoided by using OH-terminated Si (001) surfaces for the initial stage of the Al_2O_3 thin-film growth using ALD. Ghosh *et al.*[23] reported the initial mechanism of TMA for the Al_2O_3 thin-film growth on fully OH-terminated Si (001) surfaces using second order Møller-Plesset perturbation theory (MP2) with quantum mechanics/molecular mechanics (QM/MM), based on the surface results of Lee *et al.*[24] The TMA-to-*di*-methylaluminum group (DMA, $Al(CH_3)_2$) reaction and DMA-to-*uni*-methylaluminum group (UMA, $AlCH_3$) reaction required energy barriers of 0.72 eV and 0.84 eV, respectively. However, they considered only the intra-dimer site for the DMA migration because of the small surface size of 2 × 2.

In the present paper, the reaction of TMA was studied for the initial Al_2O_3 thin-film growth on fully OH-terminated Si (001) surfaces using density functional theory (DFT). A 4 × 4 surface size was used to consider the several paths of DMA migration, such as the inter-dimer, intra-dimer, and inter-dimer sites.

Calculation Details

These calculations were performed using the Vienna *ab-initio* simulation package (VASP) code with the projector augmented wave (PAW) method and the generalized gradient approximation (GGA).[25-28] The residual minimization method of direct inversion in the iterative subspace (RMM-DIIS) was used to calculate the ground state of electrons.[29,30] More precisely, Si atom $3s^2$ and $3p^2$ states, O atom $2s^2$ and $2p^4$ states, Al atom $3s^2$ and $3p^1$ states, C atom $2s^2$ and $2p^2$ states, and H atom $1s^1$ state were treated as valence wave functions. The cutoff energy was 500 eV, and the *k*-points mesh was 2 × 2 × 1, using Monkhorst-Pack for the slab superstructure with a 20 Å vacuum layer. All calculations were non-spin-polarized with the Gaussian method.

We calculated favorable adsorption sites for TMA on OH-terminated Si (001) surfaces and energy barriers for TMA reaction to produce DMA. The rotation and migration of DMA were calculated to find appropriate DMA paths. In addition, energy barriers for DMA reaction to produce UMA were compared at each site, such as the inter-dimer, inter-row, and intra-dimer sites. All energy barrier calculations were carried out using the climbing nudged elastic band (CNEB) tool.[31]

Results and Discussion

Figure 1(a) shows a planar view of a fully OH-terminated Si (001) surface. The H atoms of OH's that were attached to the Si dimers of the surface were aligned in zigzag fashion in the

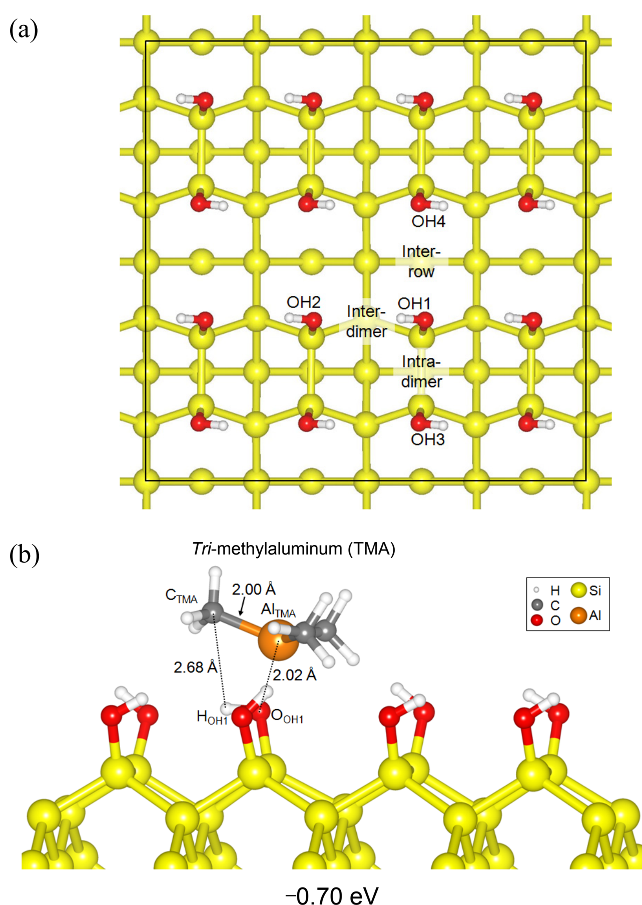

Figure 1. (a) Planar view of a fully OH-terminated Si (001) surface, shown along the [001] direction. (b) Perspective view of the adsorbed TMA on the surface, shown along the [100] direction.

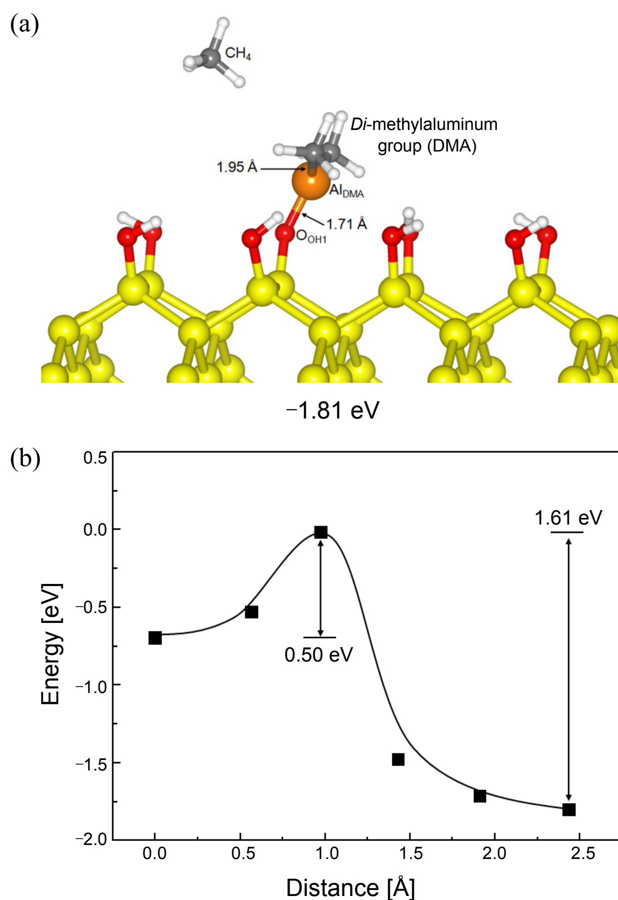

Figure 2. (a) Perspective view of the formed DMA and CH_4 along the [100] direction. (b) The energy variation as a function of the carbon ($C1_{TMA}$) distance.

same direction as that of the dimer row. Three surface sites were identified for the adsorption of TMA on the surface; Inter-dimer, intra-dimer, and inter-row sites were located between OH1 and OH2, OH1 and OH3, and OH1 and OH4, respectively. When TMA was placed on top of the surface at a distance of 10 Å, the energy of the structure was set to 0 eV as a reference. TMA approached the surface, and adsorbed onto the surface with energy decrease to −0.70 eV, as shown in Figure 1(b). More precisely, the Al atom of TMA (Al_{TMA}) was positioned on the O atom of OH1 (O_{OH1}) with an $Al_{TMA}\cdots O_{OH1}$ distance of 2.02 Å, due to the attraction induced by the lone pair electrons of O_{OH1}. As these lone pair electrons were inclined to Al_{TMA}, the H atom of OH1 (H_{OH1}) was moved away from Al_{TMA}, and a $C_{TMA}\cdots H_{OH1}$ distance was reduced to 2.68 Å.

The adsorbed TMA reacts with OH to produce DMA and methane (CH_4), and its reaction formula is given by:

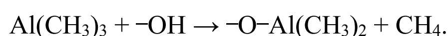

$$Al(CH_3)_3 + {-OH} \rightarrow {-O}{-Al(CH_3)_2} + CH_4.$$

One methyl (CH_3) of the adsorbed TMA reacted with H_{OH1} to produce CH_4, and thereby DMA was formed on O_{OH1}. In this case, Al_{DMA} was bonded to the O atom with a bond length of 1.71 Å, and the Al-C bond length in DMA decreased from 2.00 Å to 1.95 Å, as shown in Figure 2(a). In addition, the energy further decreased from −0.70 to −1.57 eV. An energy barrier of 0.50 eV was needed for TMA reaction to decompose CH_3 from TMA. This value was lower than the literature's value (0.72 eV[23]) because we used different theory and surface model. The reverse reaction between the formed DMA and CH_4 to produce TMA could not be plausible because of its higher energy barrier of 1.61 eV, as shown in Figure 2(b).

The formed DMA should migrate between two O atoms to react further for UMA generation. There were three different sites for DMA migration on the surface, such as the inter-dimer, intra-dimer, and inter-row sites. When DMA migrated to the inter-dimer site, as shown in Figure 3(a), the energy decreased from −1.57 to −2.18 eV. Additionally, the Al-O bond length increased from 1.71 to 1.77 Å because of the interaction between the Al atom and the neighboring O atom (O_{OH2}). O_{OH2} approached the Al atom to a distance of 2.07 Å, due to its lone pair electrons, as shown in the final-state image of Figure 3(a). In this case, the energy barrier was not required for DMA migration to the inter-dimer site. Namely, DMA was easily located at the inter-dimer site after the TMA-to-DMA reaction. DMA rotated by 90° counterclockwise with an energy barrier of 0.07 eV before it migrated to the intra-dimer and inter-row sites, and the energy decreased from −1.57 to −1.76 eV, as shown in Figure 3(b). When the rotated DMA migrated to the intra-dimer site,

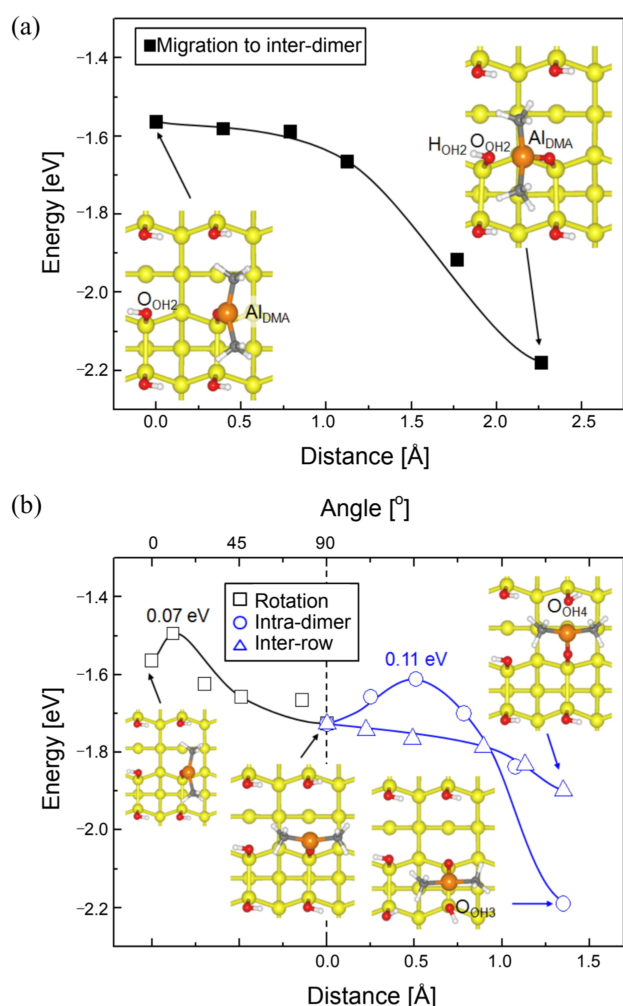

Figure 3. The energy barriers for the DMA reaction at the (a) inter-dimer site, and at the (b) intra-dimer and inter-row sites. DMA rotates by 90° before it migrates to the intra-dimer and inter-row sites while it migrates to the inter-dimer site without the rotation.

the energy decreased to −2.19 eV. The Al-O bond length also increased from 1.71 to 1.77 Å because of the interaction between the Al atom and the neighboring O atom (O_{OH3}). O_{OH3} approached the Al atom to a distance of 2.06 Å, due to its lone pair electrons. An energy barrier of 0.11 eV was needed for the rotated DMA to migrate to the intra-dimer site.[32] When DMA migrated to the inter-row site, the energy further decreased to −1.90 eV with no energy barrier. The Al-O bond length also increased to 1.77 Å, and O_{OH1} approached the Al atom to a distance of 2.24 Å.

The reaction formula between the migrated DMA and OH to produce UMA and CH_4 is given by:

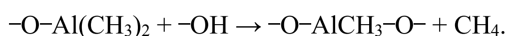

$$-O-Al(CH_3)_2 + -OH \rightarrow -O-AlCH_3-O- + CH_4.$$

One CH_3 reacted with the H atom of OH located near Al_{DMA} to produce CH_4, and thereby UMA is formed. During the reaction, the remaining CH_3 of UMA moved and became located on top of the Al atom of UMA (Al_{UMA}). When DMA reacted with OH to produce UMA and CH_4 at the inter-dimer site, as shown in Figure 4(a), the energy decreased from −2.18 to −2.89 eV. The

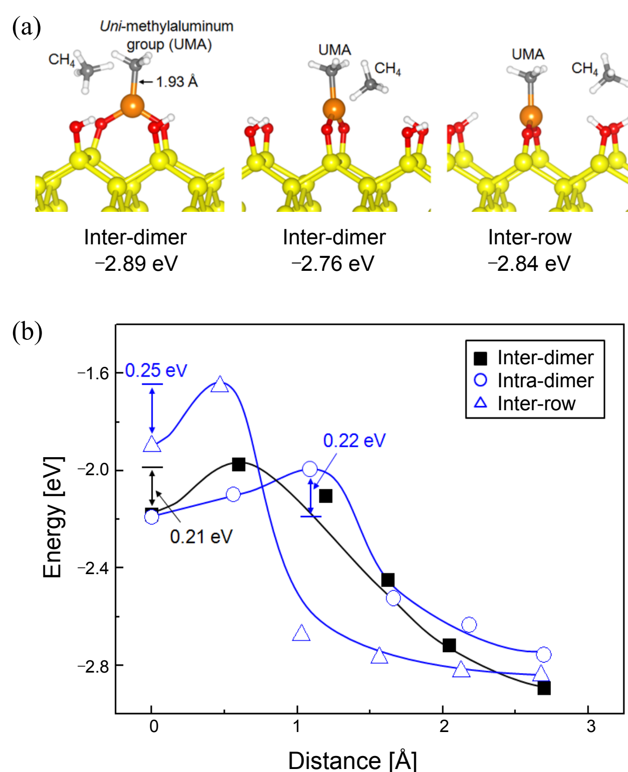

Figure 4. Perspective views of UMA located at the inter-dimer, intra-dimer, and inter-row sites from the left side along the [100] direction. (b) The energy barriers for DMA reaction to produce UMA and CH_4 at each site.

Table 1. Calculated relative probabilities of the molecules' migration and reaction at each site.

	Probability		
	Inter-dimer	Intra-dimer	Inter-row
DMA migration	1	0.005	0.13
DMA-to-UMA reaction	2.26×10^{-3}	1.69×10^{-3}	7.08×10^{-4}
Total	2.26×10^{-3}	9.12×10^{-6}	9.29×10^{-5}

Al-O bond length decreased from 1.77 to 1.73 Å, and the Al-C bond length in UMA decreased from 1.95 to 1.93 Å. When UMA was located at the intra-dimer or inter-row sites, the energy decreased to −2.76 and −2.84 eV, respectively. Both DMA-to-UMA reactions were similar to the case of the DMA-to-UMA reaction at the inter-dimer site. Figure 4(b) shows the energy barriers for the migrated DMA reaction to produce UMA and CH_4 at each site. These energy barriers were in the range of 0.21 - 0.25 eV, and were similar to each other. The relative probabilities for the molecule's migration and reaction were calculated using the Arrhenius-type equation at reaction temperature of 400 K[11], as shown in Table 1. UMA was formed most probably at the inter-dimer site among the three different sites.

Conclusion

We studied the reaction of TMA for the initial growth of Al_2O_3 thin-films on fully OH-terminated Si (001) surfaces using

DFT. The Al atom of TMA located on the O atom of OH was energetically the most favorable, due to the lone pair electrons of the O atom when TMA was adsorbed on the surface. The adsorbed TMA reacted with OH to produce DMA and CH_4 with an energy barrier of 0.50 eV. When the formed DMA migrated to the inter-dimer, intra-dimer, and inter-row sites, a neighboring O atom approached the Al atom, due to its lone pair electrons, and low energy barriers for migration in the range of 0 - 0.11 eV were required. UMA was generated at each site with energy barriers in the range of 0.21 - 0.25 eV. Among the three sites, the inter-dimer site was the most probable for UMA formation.

Acknowledgments. This work was supported by the Korea Science and Engineering Foundation (KOSFET) through the Basic Science Programs for General Research Grants (No. 2009-0076318).

References

1. Colinge, J.-P. *Solid State Electron* **2004**, *48*, 897.
2. Koh, M.; Mizubayashi, W.; Iwamoto, K.; Murakami, H.; Ono, T. *IEEE Trans. Electron Dev.* **2001**, *48*, 259.
3. Front End Processes, *International Technology Roadmap for Semiconductors*; 2003.
4. Lin, C.; Zhang, N.; Shen, Q. *Metals & Mat. Inter.* **2004**, *10*, 475.
5. Kim, W. S.; Kawahara, T.; Itoh, H.; Horiuchi, A.; Muto, A.; Maeda, T.; Mitsuhashi, R.; Torii, K.; Kitajima, H. *Jap. J. Appl. Phys.* **2004**, *43*, 1860.
6. Wilk, G. D.; Wallace, R. M.; Anthony, J. M. *J. Appl. Phys.* **2001**, *89*, 5243.
7. Klein, T. M.; Niu, D.; Epling, W. S.; Li, W.; Maher, D. M.; Hobbs, C. C.; Baumvol, I. J. R.; Parsons, G. N. *Appl. Phys. Lett.* **1999**, *75*, 4001.
8. Jeon, T. S.; White, J. M.; Kwong, D. L. *Appl. Phys. Lett.* **2001**, *78*, 368.
9. Sayan, S.; Garfunkel, E.; Nishimura, T.; Schulte, W. H.; Gustafsson, T.; Wilk, G. D. *J. Appl. Phys.* **2003**, *94*, 928.
10. Copel, M.; Cartier, E.; Gusev, E. P.; Guha, S.; Bojarczuk, N.; Poppeller, M. *Appl. Phys. Lett.* **2001**, *78*, 2670.
11. Guha, S.; Gusev, E. P.; Okorn-Schmidt, H.; Copel, M.; Ragnarsson, L.-Å; Bojarczuk, N. A.; Ronsheim, P. *Appl. Phys. Lett.* **2002**, *81*, 2956.
12. Yu, X.; Zhu, C.; Yu, M. *Appl. Phys. Lett.* **2006**, *89*, 163508.
13. Rhee, S. J.; Lee, J. C. *Microelectron. Reliability* **2005**, *45*, 1051.
14. Groner, M. D.; Fabreguette, F. H.; Elam, J. W.; George, S. M. *Chem. Mater.* **2004**, *16*, 639.
15. Ritala, M.; Kukli, K.; Rathu, A.; Raisanen, P. I.; Leskelä, M.; Sajavaara, T.; Leinonen, J. *Science* **2000**, *288*, 319.
16. Georges, S. M.; Ott, A. W.; Klaus, J. W. *J. Phys. Chem.* **1996**, *100*, 13121.
17. Ye, P. D.; Wilk, G. D.; Kwo, J.; Yang, B.; Gossmann, H.-J. L.; Chu, S. N. G.; Mannaerts, J. P.; Sergent, M.; Hong, M.; Ng, K. K.; Bude, J. *IEEE Electron Dev. Lett.* **2003**, *24*, 209.
18. Manchanda, L.; Morris, M. D.; Green, M. L.; van Dover, R. B.; Klemens, F.; Sorsch, T. W.; Silverman, P. J.; Wilk, G.; Busch, B.; Aravamudhan, S. *Microelectron. Eng.* **2001**, *59*, 351.
19. Widjaja, Y.; Musgrave, C. B. *Appl. Phys. Lett.* **2002**, *80*, 3304.
20. Heyman, A.; Musgrave, C. B. *J. Phys. Chem. B* **2004**, *108*, 5718.
21. Halls, M. D.; Raghavachari, K. *J. Phys. Chem. B* **2004**, *108*, 4058.
22. Halls, M. D.; Raghavachari, K.; Frank, M. M.; Chabal, Y. J. *Phys. Rev. B* **2003**, *68*, 161302.
23. Ghosh, M. K.; Choi, C. H. *Chem. Phys. Lett.* **2006**, *426*, 365.
24. Lee, S. S.; Baik, J. Y.; An, K. S.; Suh, Y. D.; Oh, J. H.; Kim, Y. *J. Phys. Chem. B* **2004**, *108*, 15128.
25. Kresse, G.; Hafner, J. *Phys. Rev. B* **1993**, *47*, 558; ibid **1994**, *49*, 14251.
26. Kresse, G.; Furthmüller, J. *Comput. Mat. Sci.* **1996**, *6*, 15.
27. Kresse, G.; Furthmüller, J. *Phys. Rev. B* **1996**, *54*, 11169.
28. Kresse, G.; Joubert, D. *Phys. Rev. B* **1999**, *59*, 1758.
29. Wood, D. M.; Zunger, A. *J. Phys. A* **1985**, *18*, 1343.
30. Pulay, P. *Chem. Phys. Lett.* **1980**, *73*, 393.
31. Sheppard, D.; Terrell, R.; Henkelman, G. *J. Chem. Phys.* **2008**, *128*, 134106.
32. Kim, D.-H.; Kim, D.-H.; Seo, H.-I.; Kim, Y.-C. *Trans. Electric. & Electron. Mater.* **2010**, *11*, 11.